Cloning, Overexpression, and Purification of Aminoglycoside Antibiotic Nucleotidyltransferase (2″)-Ia: Conformational Studies with Bound Substrates†

D. R. Ekman, E. L. DiGiammarino,‡ E. Wright, E. D. Witter, and E. H. Serpersu*

Department of Biochemistry and Cellular and Molecular Biology, The University of Tennessee, Walters Life Sciences Building, M407, Knoxville, Tennessee 37996-0840

Received December 13, 2000; Revised Manuscript Received April 30, 2001

ABSTRACT: Aminoglycoside nucleotidyltransferase (2″)-Ia [ANT (2″)-Ia] was cloned from *Pseudomonas aeruginosa* and purified from overexpressing *Escherichia coli* BL21(DE3) cells. The first enzyme-bound conformation of an aminoglycoside antibiotic in the active site of an aminoglycoside nucleotidyltransferase was determined using the purified aminoglycoside nucleotidyltransferase (2″)-Ia. The conformation of the aminoglycoside antibiotic isepamicin, a psuedo-trisaccharide, bound to aminoglycoside nucleotidyltransferase (2″)-Ia has been determined using NMR spectroscopy. Molecular modeling, employing experimentally determined interproton distances, resulted in two different enzyme-bound conformations (conformer 1 and conformer 2) of isepamicin. Conformer 1 was by far the major conformer defined by the following average glycosidic dihedral angles: $\Phi_{BC} = -65.26 \pm 1.63°$ and $\Psi_{BC} = -54.76 \pm 4.64°$. Conformer 1 was further subdivided into one major (conformer 1a) and two minor components (conformers 1b and 1c) based on the comparison of glycosidic dihedral angles Φ_{AB} and Ψ_{AB}. The arrangement of substrates in the enzyme·metal-ATP·isepamicin complex was determined on the basis of the measured effect of the paramagnetic substrate analogue $Cr(H_2O)_4ATP$ on the relaxation rates of substrate protons which were used to determine relative distances of isepamicin protons to the Cr^{3+}. Both conformers of isepamicin yielded arrangements that satisfied the NOE restraints and the observed paramagnetic effects of $Cr(H_2O)_4ATP$. It has been suggested that aminoglycosides use both electrostatic interactions and hydrogen bonds in binding to RNA and that the contacts made by the A and B rings to RNA are the most important for binding [Fourmy, D., Recht, M. I., Blanchard, S. C., and Puglisi, J. D. (1996) *Science 274*, 1367−1371]. Comparisons based on the determined conformations of enzyme-bound aminoglycoside antibiotics also suggested that interactions of rings A and B with enzymes may be the major determinant in aminoglycoside binding to enzymes [Serpersu, E. H., Cox, J. R., DiGiammarino, E. L., Mohler, M. L., Ekman, D. R., Akal-Strader, A., and Owston, M. (2000) *Cell Biochem. Biophys*. (in press)]. The conformation of isepamicin bound to the aminoglycoside nucleotidyltransferase (2″)-Ia, determined in this work, lent further support to this theory. Furthermore, comparison of enzyme-bound conformations of isepamicin to the RNA-bound conformation of gentamycin C_{1a} also showed remarkable similarities between the enzyme-bound and RNA-bound aminoglycoside antibiotic conformations. These studies should aid in the design of effective inhibitors possessing a broad range of aminoglycoside-modifying enzymes as targets.

Bacterial resistance to the existing armamentarium of antibiotics has both the medical community and the scientific community in a state of alarm. One class of antibiotics, in particular, that has experienced extensive resistance is the aminoglycosides, which are primarily known for their effectiveness in the treatment of serious Gram-negative bacterial infections. The majority of aminoglycosides target the prokaryotic 16S ribosomal RNA of the 30S subunit and inhibit the process of translation (*1*, *2*). Using a mechanism that is largely unknown, the extensive damage resulting from this inhibition eventually leads to cell death. However, resistance mechanisms exist which can interfere with this bactericidal interaction. Enzymatic modification of aminoglycosides represents the major mechanism of resistance to the aminoglycoside antibiotics (*3*, *4*). Three different types of aminoglycoside-modifying enzymes have been described: the *O*-phosphotransferases (APHs), the *N*-acetyltransferases (AACs), and the *O*-nucleotidyltransferases (ANTs) (*4*, *5*). More than 50 different enzymes encompassing all three classes have been identified. In addition, many individual enzymes have the ability to modify a wide variety of different aminoglycoside antibiotics. It is clear that more effective antibiotics and potential inhibitors of the modification enzymes need to be developed to combat antibiotic resistance effectively. This task would be aided by a more detailed knowledge of chemical and biological interactions between the aminoglycoside-modifying enzymes and their substrates. Thus, determination of the conformations of

† This work was supported by a grant from the Petroleum Research Fund (32874-AC4 to E.H.S.).

* To whom correspondence should be addressed. Telephone: (423) 974-2668. Fax: (423) 974-6306. E-mail: eserpersu@utk.edu.

‡ Present address: Department of Structural Biology, St. Jude Children's Research Hospital, 332 N. Lauderdale, Memphis, TN 38105.

10.1021/bi002827b CCC: $20.00
Published on Web 05/25/2001

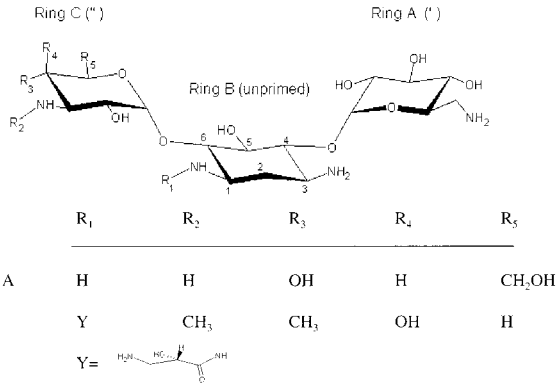

FIGURE 1: Structures of aminoglycoside antibiotics kanamycin A and isepamicin. Both aminoglycosides contain a 4,6-disubstituted 2-DOS ring (ring B).

enzyme-bound antibiotics would be an important step toward this goal.

Crystal structures of several aminoglycoside-modifying enzymes have been determined, but these structures did not reveal conformations of enzyme-bound antibiotics (*6*−*10*). Enzyme-bound conformations of several aminoglycoside antibiotics have been determined by NMR (*11*−*17*). However, there are no data available on the conformation of an aminoglycoside bound to an enzyme in the aminoglycoside nucleotidyltransferase group. This paper describes the cloning, overexpression, and purification of aminoglycoside nucleotidyltransferase (2″)-Ia [ANT (2″)-Ia][1] as well as the determination of an enzyme-bound aminoglycoside conformation.

ANT (2″)-Ia has been recognized as being widespread among all Gram-negative bacteria and is the most common enzyme responsible for the aminoglycoside resistance in North America (*5*, *18*). It confers resistance through a mechanism involving regiospecific transfer of a nucleoside monophosphate to the 2C (or 2″) hydroxyl of the aminoglycoside substrates in its resistance profile as shown below.

$$\text{MgATP} + \text{2″-hydroxyaminoglycoside} \rightarrow \text{MgPP}_i + \text{AMP-2″-aminoglycoside}$$

Although kinetic and crystallographic studies were performed with two different nucleotidyltransferases (*7*, *18*−*22*), the conformation of a bound aminoglycoside in the active site of a nucleotidyltransferase is not known. In this paper, we report cloning, overexpression, and purification of ANT (2″)-Ia, as well as the first nucleotidyltransferase-bound conformation of an aminoglycoside antibiotic.

EXPERIMENTAL PROCEDURES

Materials. Kanamycin A (Figure 1) was from Sigma Chemical Co. Isepamicin (Figure 1) was a gift from K. Shaw and G. Miller of Schering Plough, and deuterated ethylene glycol, glycerol, DTT, and Tris were from Isotec, Inc.

Cloning. The gene for ANT (2″)-Ia was obtained from a *Pseudomonas aeruginosa* clinical isolate using standard PCR procedures. The clinical isolate of this organism was kindly provided by K. Shaw of Schering Plough. The ANT (2″)-Ia gene was inserted into the pET-22b(+) vector and transformed into *Escherichia coli* strain BL21(DE3) which then showed the expected resistance pattern to the aminoglycoside antibiotics consistent with the expression of ANT (2″)-Ia. DNA sequencing also confirmed the insertion of the ANT (2″)-Ia gene into the pET-22b(+) vector. High expression levels of ANT (2″)-Ia were observed in the form of inclusion bodies. Expression of the enzyme in soluble form was sought by using several other expression systems. Although some success was obtained in increasing the amount of soluble enzyme, in all cases the major portion (>80%) of the enzyme was still expressed in the form of inclusion bodies. Therefore, a procedure was devised to recover the active enzyme from inclusion bodies.

Isolation of ANT (2″)-Ia. Cells were lysed by passing them through a French press, and the inclusion bodies were pelleted by centrifugation at 30000*g*. The pellet was then washed using a solution of 5 mM Tris-HCl (pH 8.0) and 1% Triton X-100. The enzyme was resolubilized from the washed inclusion bodies in 8 M urea at 37 °C with shaking. Any insoluble material was pelleted, and the recovery from the denaturant was performed by carefully pipetting the solubilized protein into a stirred solution of 10 mM HEPES, 0.125 mM EDTA, 10 mM DTT, 1% glycerol, 0.5% ethylene glycol, 1 mM magnesium acetate, and 50 mM KCl at pH 8.0. The enzyme concentration was 0.25 mg/mL in the recovery medium. The solution, containing the recovered enzyme, was then concentrated using ultrafiltration. The molecular weight of the purified ANT (2″)-Ia was determined to be 25 590 from the amino acid sequence of the protein which was also confirmed by mass spectrometry.

Assay for Activity of ANT (2″)-Ia. The activity of ANT (2″)-Ia was determined using an assay based on the determination of the amount of inorganic phosphate (*23*). The enzyme was incubated in a solution containing 20 mM Tris-HCl (pH 8.4), 2.5 mM ATP, 5 mM $MgCl_2$, isepamicin, 50 mM KCl, and 10 mM DTT. Inorganic pyrophosphatase (2.5 units) was also included in assays to ensure the complete conversion of the reaction product pyrophosphate to the inorganic phosphate. After incubation at 37 °C, the reaction was stopped by the addition of $HClO_4$ at a final concentration of 4%. The level of inorganic phosphate was determined using an aliquot of the supernatant. V_{max} values of 5.8 μmol min^{-1} mg^{-1} with kanamycin A and 0.36 μmol min^{-1} mg^{-1} with isepamicin were determined. The K_m values for kanamycin A and isepamicin were 180 and 310 μM, respectively. $K_{m-MgATP}$ was determined to be 1.2 mM. These values are similar to those reported for different nucleotidyltransferases, and the enzyme turnover rate (2−3 s^{-1}) is in excellent agreement with the rates of other aminoglycoside-modifying enzymes.

Purification of Modified Kanamycin. To confirm the identity of the reaction product, a large-scale enzymatic reaction was performed using kanamycin A as the aminoglycoside substrate. Adenylated kanamycin A was isolated using a similar procedure described for the adenylated tobramycin (*24*) from a reaction mixture that contained 5 mg of ANT (2″)-Ia, 10 mM ATP, 12 mM $MgCl_2$, and 100 μM kanamycin A in 50 mM Tris-HCl (pH 8.0) containing 1 mM DTT in a total volume of 100 mL. The solution was incubated at 37 °C overnight. The next morning, 2 mg of ANT (2″)-Ia was

[1] Abbreviations: ANT (2″)-Ia, aminoglycoside nucleotidyltransferase (2″)-Ia; 2-DOS, 2-deoxystreptamine; AAC (6′)-Ii, aminoglycoside acetyltransferase (6′)-Ii; APH (3′)-IIIa, aminoglycoside phosphotransferase (3′)-IIIa.

added to the solution, and the incubation was continued for an additional 4 h. The adenylated product was isolated using a procedure similar to that reported by Van Pelt et al. (*24*) for the isolation of adenylated tobramycin. The reaction product was identified by one- and two-dimensional NMR spectroscopy.

NMR Spectroscopy. Protonated solutes in the enzyme solution as well as water were replaced by deuterated counterparts using a series of dilutions and concentrations in an ultrafiltration unit. Samples for NOESY experiments contained 0.1−0.2 mM enzyme and appropriate concentrations (up to 2 mM each) of substrates ATP, $CaCl_2$, and isepamicin to achieve isepamicin-to-enzyme ratios ranging from 6 to 12. Solutions also contained 2−4 mM d_{11}-Tris-DCl (pH* 8.0, uncorrected pH meter reading), 5 mM d_{10}-DTT, 1% d_8-glycerol, and 0.5% d_6-ethylene glycol. $CaCl_2$, instead of $MgCl_2$, was used to prevent catalysis. The enzyme activity was checked after NMR experiments and found to be greater than 90% of the initial activity. No degradation of the substrates or any other spectral changes were observed during the NOE experiments.

All experiments were performed on a 600 MHz Varian Inova spectrometer equipped with a single-gradient axis and a triple-resonance probe for the observation of proton, carbon, and nitrogen nuclei. A total of 228−256 FIDs of 1408 complex data points were collected. The spectral width was 5479 Hz, and 80−128 scans per FID were acquired. Mixing times of 30, 60, and 90 ms were used in TRNOESY experiments with enzyme-bound isepamicin. The data were multiplied by a sine-squared window function in both dimensions before Fourier transformation. Similar parameters were used in the ROESY and QUIET-NOESY experiments. A Gaussian Cascade Q3 pulse was used in the middle of the mixing period, for the selective inversion of different substrate protons, in the QUIET-NOESY experiments (*25*, *26*). QUIET-NOESY experiments were repeated with the systematic inversion of different parts of the isepamicin proton spectrum, which suggested that there was no significant spin diffusion.

Distance Calculations. The intensities of the TRNOE cross-peaks were used to assign interproton distance restraints as follows: 2.0−2.7 Å for strong, 2.0−3.6 Å for medium, and 2.0−4.5 Å for weak. These distances were assigned on the basis of the intensity of a known interproton distance ($H1_A-H2_A$, 2.38 Å).

Molecular Dynamics and Minimization. Isepamicin was constructed with Insight II (BIOSYM/Molecular Simulations) operating on a Silicon Graphics Indigo-2 workstation. All calculations were carried out using the AMBER force field (*27*) interfaced with the molecular mechanics software DISCOVER (BIOSYM/Molecular Simulations) on the same workstation. The atom potential types and charges were set according to Homan's potential types for carbohydrates (*28*) in the AMBER force field. The amine groups of isepamicin were given a formal charge of +1.00, consistent with the pK_a values reported previously (*15*).

Determination of the Enzyme-Bound Conformation of Isepamicin. Restrained simulated annealing was used to obtain conformations of isepamicin in a manner similar to that described previously (*13*−*16*). Prior to simulated annealing, a set of random structures was generated by subjecting an isepamicin molecule to unrestrained dynamics at 600 K for 10.0 ps. The distance restraints obtained through TRNOESY were then imposed upon the randomized structures, and they were carried through a restrained simulated annealing scheme using restrained conjugate gradient minimizations (500 iterations) followed by restrained molecular dynamics (10.0 ps) at 450 K. This was then repeated at temperatures of 400, 350, and finally 300 K followed by a final restrained conjugate gradient minimization until the rms derivative was less than 0.001 kcal/Å. The restraints were then removed, and the structure was subjected to molecular dynamics at 100 K (10.0 ps) followed by a final conjugate gradient minimization until the rms derivative was less than 0.001 kcal/Å. All simulations were carried out using a dielectric constant of 4.0 in vacuo which was prescribed by the Discover module for structure calculations of carbohydrates with the AMBER force field. An energetic penalty of 50 kcal mol^{-1} $Å^{-2}$ was used for violation of the distance restraints.

RESULTS AND DISCUSSION

Cloning, Overexpression, and Isolation of ANT (2″)-Ia. Once cloned and transformed into genetically engineered *E. coli*, large quantities (20−30 mg/L) of purified ANT (2″)-Ia could easily be obtained using the isolation procedure described above. The recovered enzyme (>95% pure, judged by SDS gel electrophoresis) displayed k_{cat} values of 2−3 s^{-1} using kanamycin A and MgATP as substrates. These values are well within the range of values obtained with other aminoglycoside-modifying enzymes. Both the quantity and purity of this enzyme now permit more structurally based studies to be conducted.

Although the antibiotic resistance pattern of *E. coli* as well as the DNA sequence of the cloned enzyme matched the expected profile of ANT (2″)-Ia, the point of chemical modification on an aminoglycoside was determined by using kanamycin A as the substrate. One- and two-dimensional NMR experiments showed that the purified reaction product was adenylated kanamycin A at the 2″-OH.

ANT (2″)-Ia-Bound Conformations of Isepamicin. A total of 25 TRNOEs were observed for isepamicin bound to ANT (2″)-Ia. Of these 25 NOEs, 21 were intraring and served to define the conformations of the individual rings, while the remaining four TRNOEs were inter-ring and thus provided information about the relative orientation of rings with respect to each other. Particularly important for defining the conformation of the rings with respect to one another were the inter-ring TRNOEs that were observed across the glycosidic bonds. Figure 2 shows the region of a TRNOESY spectrum where inter-ring TRNOEs were observed. The intensities of the observed NOE cross-peaks were sorted as strong, medium, and weak on the basis of the determined volumes, and assigned to distance ranges of 2.0−2.7, 2.0−3.6, and 2.0−4.5 Å, respectively. The intensities of TRNOE cross-peaks were mostly unchanged (within error) in QUIET-NOESY experiments with the exception of the cross-peak between protons $H1_A$ and $H3_B$ which exhibited slightly lower intensity in the QUIET-NOESY spectra. However, this did not affect the category of the distance restraint for this pair because the $H1_A-H3_B$ NOE was already set as a weak NOE. This observation suggests that the intensities of the observed NOE cross-peaks were not affected significantly by spin

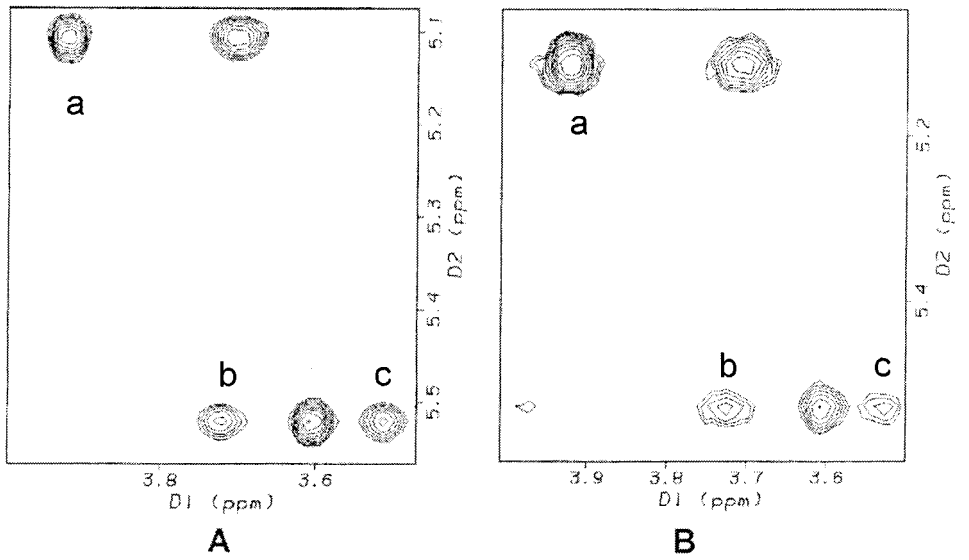

FIGURE 2: Part of the TRNOE (A) and QUIETNOESY (B) spectra for enzyme-bound isepamicin. Both spectra were acquired with a mixing time of 60 ms on a 600 MHz Varian spectrometer. The top and bottom rows represent TRNOEs that were observed with $H1_C$ and $H1_A$, respectively. Some important cross-peaks are marked: $H1_C-H6_B$ (a), $H1_A-H4_B$ (b), and $H1_A-H3_B$ (c). The NMR sample contained 0.15 mM ANT (2″)-Ia, 1 mM isepamicin, 1 mM ATP, 1 mM $CaCl_2$, 1% d_8-glycerol, 0.5% d_6-ethylene glycol, and 5 mM d_{10}-DTT in 4 mM d_{11}-Tris buffer (pH 8.0). A total of 256 FIDS of 1408 complex data points were collected. The spectral width was 5479 Hz, and 128 scans per FID were acquired. The data were multiplied by a sine-squared window function in both dimensions before Fourier transformation. All the NMR data were processed with Varian software.

Table 1: NMR Data and Structures

no. of distance restraints	
total	25
inter-ring	4
strong (2.0−2.7 Å)	5
medium (2.0−3.6 Å)	5
weak (2.0−4.5 Å)	15
pairwise rmsd (Å) among the final structures	
ring B and C heavy atoms	
all structures	0.240 ± 0.419
conformer 1	0.06475 ± 0.051
conformer 2	0.047 ± 0.0127
ring A and B heavy atoms only	
all structures	0.370 ± 0.383
conformer 1	0.327 ± 0.3925
conformer 1a	0.0488 ± 0.0283
conformer 1b	0.066 ± 0.0828
conformer 1c	0.016 ± 0.0026
conformer 2	0.037 ± 0.013
isepamicin bound to three different enzymes	0.0865 ± 0.025
glycosidic (BC) angles for both conformers	
Φ_{BC} (degs)	
conformer 1	−65.26 ± 1.63
conformer 2	−41.05 ± 0.88
Ψ_{BC} (deg)	
conformer 1	−54.76 ± 4.64
conformer 2	61.15 ± 0.616

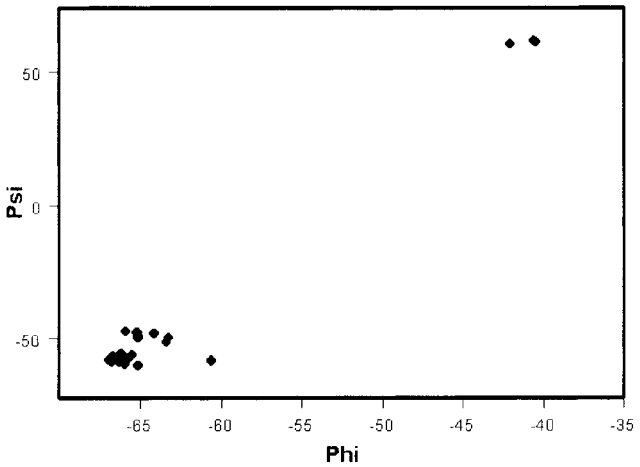

FIGURE 3: Φ_{BC} vs Ψ_{BC} plot for conformer 1 and conformer 2 of isepamicin.

diffusion due to the presence of nearby protein protons (unless they exactly overlap with the resonances of interest).

A total of 23 acceptable structures were obtained from the restrained simulated annealing performed by using the NOE distance restraints. These structures were first evaluated on the basis of the orientation of the C ring with respect to the 2-DOS ring since the C ring is the site of modification by ANT (2″)-Ia. Two conformers (conformer 1 and conformer 2) emerged from this comparison. The conformers could be distinguished from each other by comparing the pairwise rmsd values from the superimposition of the B and C rings (Table 1), and by measurement of the glycosidic dihedral Φ_{BC} ($H1_C-C1_C-O_a-C6_B$) and Ψ_{BC} ($H6_B-C6_B-O_a-C1_C$) angles (Table 1 and Figure 3). The clustering of the structures is clearly visible in a plot of Φ_{BC} versus Ψ_{BC} as shown in Figure 3. Conformer 1 was determined to be the major conformer containing 20 structures, while conformer 2 was considered to be the minor conformer containing only three structures (Figure 4).

It is known that the aminoglycosides make the most important contacts with RNA through the A and B rings (*29*, *30*). It has also been suggested that binding to aminoglycoside-modifying enzymes may also be primarily determined by the A and B rings (*17*). However, it is not clear whether this is still true for enzymes such as ANT (2″)-Ia which modifies the C ring of aminoglycosides. Therefore, we made comparisons on the basis of the conformations of the A and B rings using the conformation of isepamicin determined in this work. To aid in comparison, we evaluated conformer 1 on the basis of the orientation of ring A with respect to the 2-DOS ring. Although, as seen in Figure 4, the A ring of isepamicin appears not to be well defined and can adopt different orientations with respect to the 2-DOS ring, further

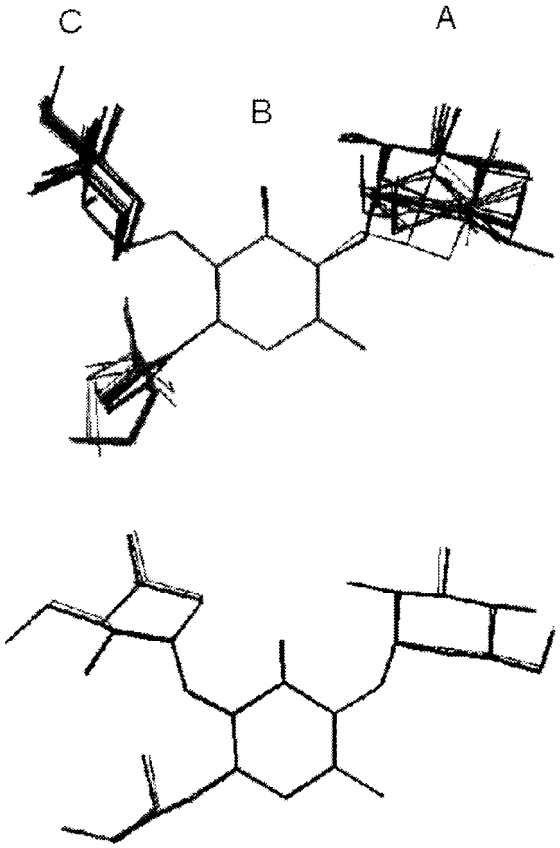

FIGURE 4: ANT (2″)-Ia-bound conformations of isepamicin. Comparisons were based on superpositioning of ring B and ring C to yield the minimum rmsd. Conformer 1 is shown at the top.

subdivision of conformer 1 into three different conformers [conformer 1a (12 structures), conformer 1b (five structures), and conformer 1c (three structures)] was possible on the basis of the orientations of the A ring relative to the B ring (Figure 5). As shown in Table 1, the average rmsd values dropped significantly from those seen for all the structures in conformer 1. It is interesting to note that conformer 2 looks very similar to conformer 1a based on this comparison. It is also possible that the subconformers of conformer 1 were observed due to the lack of a large number of inter-ring NOE restraints (two in this case), and some of them may simply represent conformations that satisfy the restraints but not necessarily occur in solution. Lack of inter-ring NOE restraints has been a frequent problem observed with carbohydrates.

If one assumes that the A and B rings of isepamicin play a major role in binding, then the superimposition of conformers 1 and 2 through these rings would position the reactive hydroxyl group about 2.1 Å shifted within the active site of ANT (2″)-Ia. Upon searching for sites of potential hydrogen bonding within the molecule, we found conformer 1a displayed a potential hydrogen bond between the 2-OH of the A ring and the 5-OH of the B ring. Conformer 1b also displayed a possible hydrogen bond between the A and B rings but from the 6-NH_2 of the A ring to the 3-NH_2 of the B ring. No hydrogen bonds were observed for conformer 1c. If the conformations involving the A and B rings are the major determinants in binding, then the superimposition of conformer 1a and conformer 2 about these rings would place the C ring of each conformer into a different position. Thus, although both conformers may bind to ANT (2″)-Ia in a

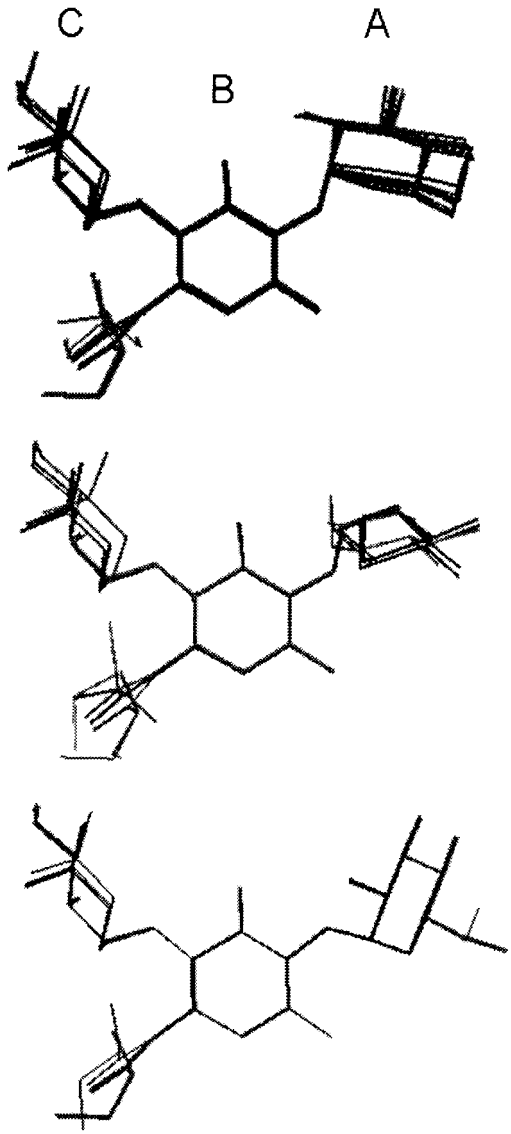

FIGURE 5: Three subconformers of conformer 1 based on the comparison of rings A and B. From top to bottom: conformer 1a, conformer 1b, and conformer 1c.

similar fashion with respect to their A and B rings, the orientation of the C ring in one of them may not be suitably positioned for catalysis. This may cause isepamicin to bind to the enzyme in an unproductive manner, and it may be one of the key factors for its clinical efficacy. If the antibiotic binds in a manner unsuitable for catalysis, it may decrease the enzyme's efficiency by spending a greater amount of time occupying its active site and allowing other unmodified drugs to move into the cell unaffected.

Unrestrained molecular dynamics at 300 K was performed for 1 ns starting from one of the final structures representing each conformer. Trajectories of the Φ_{BC} and Ψ_{BC} angles defining the orientation of the B and C rings were obtained over this time period to determine whether the two conformers could interconvert. Ψ_{BC} of conformer 2 quickly converted into the value recognized for conformer 1a and then did not convert back. On the other hand, when we started from conformer 1a, Ψ_{BC} did not convert to that of conformer 2 (the Φ angle differences between conformer 1a and conformer 2 were small compared to the differences in the Ψ angles). This is consistent with the observation that con-

former 1a emerged as the major conformer from the restrained simulated annealing. The vast majority of values for the structures in conformer 1a did in fact display lower energy values when compared to those that were measured for conformer 2. If one assumes that conformer 1 represents the conformation of the antibiotic in the productive enzyme−antibiotic complex, then conformer 2 represents either a structure which satisfies the TRNOE restraints but does not necessarily represent a bound conformation or another enzyme-bound conformation that quickly converts to conformer 1. It should be mentioned that the time required for a single catalytic turn for ANT (2″)-Ia (∼0.4 s with kanamycin A) is much longer than the duration of the molecular dynamics simulation. Thus, the interconversion of conformer 2 to conformer 1 is plausible during catalysis. Alternatively, if the interconversion in the active site may be prevented by steric hindrance, then conformer 2 may represent the formation of an unproductive enzyme−substrate complex.

Arrangement of Substrates in the Active Site of ANT (2″)-Ia. Measurement of the paramagnetic relaxation rates ($1/T_{1p}$) of substrate magnetic nuclei (protons), in the presence of a paramagnetic probe, allows for the calculation of distances from the ^{1}H nuclei of an enzyme-bound molecule in solution to a paramagnetic center (*31*, *32*). Information about the conformation and arrangement of enzyme-bound substrates can be derived from distances determined in this manner. To provide an independent test for the conformations determined by NOE distance restraints, we used paramagnetic β,γ-bidentate $Cr(H_2O)_4ATP$ (CrATP) to determine distances between several protons of isepamicin and Cr^{3+}. CrATP is a stable exchange-inert metal-ATP analogue, which has been used as a paramagnetic probe for intersubstrate distance measurements (*12*, *33*−*35*).

The paramagnetic effect of CrATP on the relaxation rates of several antibiotic protons was measured to determine Cr^{3+}−^{1}H distances in the ternary ANT (2″)-Ia·CrATP·isepamicin complex. Titration of CrATP into a solution containing isepamicin and ANT (2″)-Ia resulted in an increase in the $1/T_1$ values of the antibiotic protons. Similar titrations were carried out in the absence of ANT (2″)-Ia, to correct for the effects of free CrATP and the binary CrATP·isepamicin complex. Comparison of the paramagnetic effects of CrATP on the $1/T_1$ values of the antibiotic protons in the binary CrATP·antibiotic and ternary enzyme·CrATP·antibiotic complexes shows that the presence of ANT (2″)-Ia causes an enhancement of the paramagnetic effects. The corrected and normalized paramagnetic effects ($1/fT_{1p}$) were then used to determine the relative proximity of several isepamicin protons to Cr^{3+} (Figure 6). These results showed relative distances from Cr^{3+} are in the following order: H1″, $H2_{ax}$, $H2_{eq}$ > H1′ > H3″(Me) > H2‴ (side chain at N1). These distances are depicted in Figure 7.

The relative distances used to construct the enzyme-bound arrangement, presented in Figure 7, allowed the phosphorus atom of the α-phosphoryl group of ATP to be placed approximately 4 Å from the oxygen atom of the 2″-OH group. Therefore, direct transfer of the nucleotidyl group from ATP to isepamicin is feasible. This restraint was imposed on the basis of the results of an earlier study which showed that a direct nucleophilic attack on the α-phosphorus is the most likely mechanism for the nucleotidyl transfer reaction (*36*).

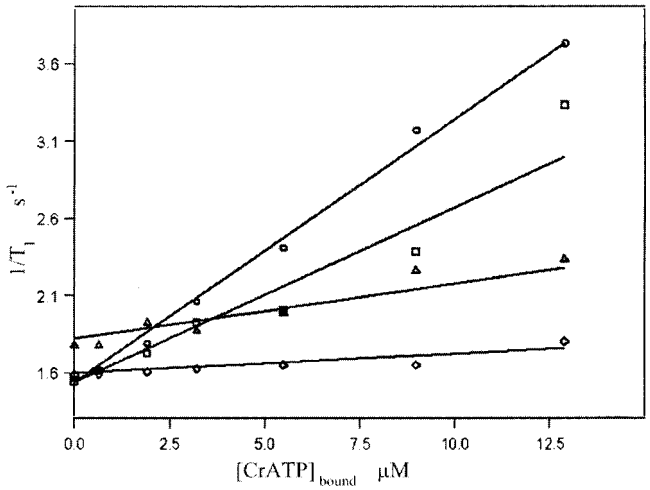

FIGURE 6: Paramagnetic affects of CrATP on the relaxation rates of isepamicin protons in the ternary enzyme·CrATP·isepamicin complex. The data are presented after correction to remove contributions due to the presence of a small amount of a binary CrATP·isepamicin complex. Curves represent the paramagnetic effects of CrATP on the longitudinal relaxation of H2‴ (○), H3″-(Me) (□), H1′ (△), and H1″, $H2_{ax}$, and $H2_{eq}$ (◇). Due to similarity, H1″, $H2_{ax}$, and $H2_{eq}$ were all represented by one curve which was shifted down for $H2_{ax}$ and $H2_{eq}$ for a more convenient presentation.

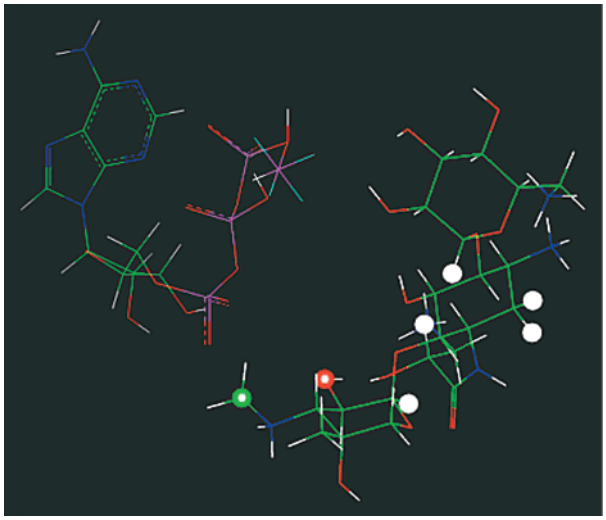

FIGURE 7: Arrangement of substrates in the active site of ANT (2″)-Ia. The 2″-OH of isepamicin is shown as a red ball, which is less than 4.5 Å from the α-phosphorus of CrATP. All the other balls represent the protons of isepamicin that satisfy the following order of relative distances: H1″, $H2_{ax}$, $H2_{eq}$ > H1′ > H3″(Me) > H2‴.

The arrangement shown in Figure 7 is constructed with conformer 1a of isepamicin. During the docking process, conformer 1a was treated as a rigid molecule and no changes in its conformation were made (except the APH side chain at N1 which rotates freely). Therefore, the arrangement and isepamicin conformation shown in this figure satisfy all the distance restraints obtained from two independent experiments. Similar arrangements were also possible with the other conformers with minor violations of one or two restraints.

Comparisons of Enzyme-Bound Conformations of Isepamicin. Conformer 1a was the major conformer that emerged from restrained simulated annealing. Comparison of this

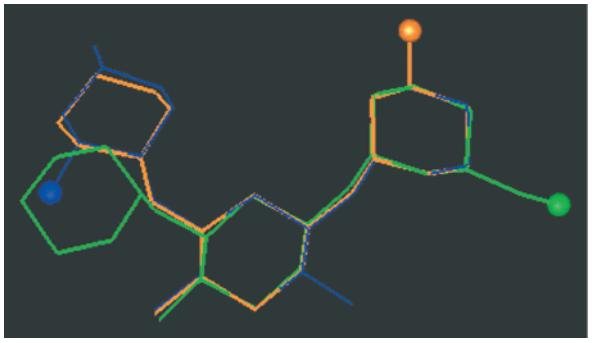

FIGURE 8: Major conformations of isepamicin, determined in the active sites of three different aminoglycoside-modifying enzymes: APH (3′)-IIIa (orange), AAC (6′)-Ii (green), and ANT (2″)-Ia (blue). All structures were superimposed to yield the minimum rmsd for the heavy atoms of rings A and B. Balls represent the sites of modification by the enzymes.

conformation to the conformations of isepamicin in the active sites of an aminoglycoside acetyltransferase-6′-Ii [AAC (6′)-Ii] (*15*) and an aminoglycoside phosphotransferase-3′-IIIa [APH (3′)-IIIa] (16) revealed distinct similarities in the orientation of the A and B rings. Superimposition of these rings produces striking agreement in their conformations with an rmsd value of 0.0865 ± 0.025 (Table 1 and Figure 8). These results support the idea that the A and B rings may contribute to binding to all aminoglycoside-modifying enzymes by providing important intermolecular contacts. The orientations of the A and B rings probably allow specific positioning of the potential hydrogen bond donors and acceptors that may often be required for binding to aminoglycoside-modifying enzymes. There are hydroxyl groups at positions 2−4 on the A ring of isepamicin and an amine group at position 6. These all most likely present necessary binding contacts (possibly electrostatic in the case of the amines) to the enzymes, and thus, they must orient correctly. In addition, the amine at position 3 of ring B, common to many of the aminoglycosides, is also probably utilized in binding and so must be presented in a manner similar to that of the three different enzymes.

It should also be mentioned that ribostamycin, an aminoglycoside with a 4,5-substituted 2-DOS ring, exhibits an A and B ring orientation similar to those mentioned above when bound to the aminoglycoside 3′-phosphotransferase-IIIa (*16*). Thus, it may be that aminoglycosides with a 4,5-disubstituted deoxystreptamine ring also bind in a similar fashion despite structural differences. Additional contacts that the C ring can make with the active site residues may serve to enhance binding but are not entirely necessary. However, it should be noted that none of the aminoglycosides with a 4,5-substituted DOS ring are substrates for ANT (2″)-Ia. This may be due to either a steric clash of the C ring with the enzyme side chains or the 2″-OH positioned incorrectly for catalysis.

Comparisons of Enzyme-Bound and RNA-Bound Aminoglycosides. The comparison described above suggests that the same aminoglycoside binds to different enzymes in remarkably similar conformations. Similarities in conformation can be extended further to the conformations of aminoglycosides bound to nonenzymatic targets such as RNA. In Figure 9, the enzyme-bound conformations of isepamicin and APH-bound conformation of ribostamycin are shown with the RNA-bound conformations of gentamycin

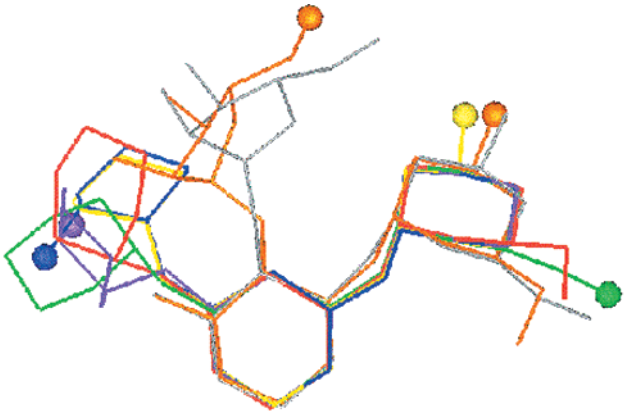

FIGURE 9: Comparison of aminoglycoside-modifying enzyme-bound and RNA aptamer-bound conformations of aminoglycosides. ANT (2″)-Ia-bound isepamicin conformer 1a (purple) and conformer 2 (blue) (this work), AAC (6′)-Ii-bound isepamicin (green) (*15*), APH (3′)-IIIa-bound isepamicin (yellow) (*16*), APH (3′)-IIIa-bound ribostamycin (orange) (*16*), RNA aptamer-bound gentamycin C_{1a} (red) (*35*), and RNA aptamer-bound paromomycin (gray) (*36*). In the enzyme-bound structures, balls represent the sites of modification by the enzymes. Rings A and B were superimposed to yield a minimum rmsd value.

C_{1a} (4,6-substituted 2-DOS ring) and paromomycin (4,5-substituted 2-DOS ring). It is clear from this comparison that all of these aminoglycosides show remarkably similar conformations about the A and B rings regardless of the substitution pattern of ring B (2-DOS ring). It has already been shown that rings A and B make the most important contacts with RNA (*29*, *30*). If this is also true for the enzyme-bound aminoglycosides, then it appears as though the aminoglycoside-modifying enzymes may have evolved their active site to emulate the chemical environment of the aminoglycoside-binding site on the 16S rRNA target. Therefore, it seems possible that the similar contacts for aminoglycoside binding to RNA are utilized in aminoglycoside−enzyme interactions. This information should aid in the design of new drugs against infectious diseases.

ACKNOWLEDGMENT

We are grateful to Drs. Michelle Buchanan and Robert Hettich of Oak Ridge National Laboratories (Oak Ridge, TN) for the mass spectrometry studies of ANT (2″)-Ia. We also thank Dr. David C. Baker of The University of Tennessee Chemistry Department for useful suggestions and discussions.

REFERENCES

1. Davies, J. E. (1991) in *Antibiotics in Laboratory Medicine* (Lorian, V., Ed.) pp 691−713, Williams and Wilkins, Baltimore.
2. Moazed, D., and Noller, H. F. (1987) *Nature 327*, 389−394.
3. Davies, J. (1994) *Science 264*, 375−382.
4. Umezawa, H. (1974) in *Advances in Carbohydrate Chemistry and Biochemistry* (Tipson, R. S., and Horton, D., Eds.) pp 183−225, Academic Press, New York.
5. Shaw, K. J., Rather, P. N., Hare, R. S., and Miller, G. H. (1993) *Microbiol. Rev. 57*, 138−163.
6. Sakon, J., Liao, H. H., Kanikula, A. M., Benning, M. M., Rayment, I., and Holden, H. M. (1993) *Biochemistry 32*, 11977−11984.
7. Pedersen, L. C., Benning, M. M., and Holden, H. M. (1995) *Biochemistry 34*, 13305−13311.

8. Hon, W.-C., McKay, G. A., Thompson, P. R., Sweet, R. M., Yang, D. S. C., Wright, G. D., and Berghuis, A. M. (1997) *Cell 89*, 887−895.
9. Wolf, E., Vassilev, A., Makino, Y., Sali, A., Nakatani, Y., and Burley, S. K. (1998) *Cell 94*, 439−449.
10. Wybenga-Groot, L., Draker, K.-a., Wright, G., and Berghuis, A. M. (1999) *Structure 7*, 497−507.
11. Cox, J. R., and Serpersu, E. H. (1995) *Carbohydr. Res. 271*, 55−63.
12. Cox, J. R., McKay, G. A., Wright, G. D., and Serpersu, E. H. (1996) *J. Am. Chem. Soc. 118*, 1295−1301.
13. Cox, J. R., and Serpersu, E. H. (1997) *Biochemistry 36*, 2353−2359.
14. Mohler, L. M., Cox, J. R., and Serpersu, E. H. (1997) *Carbohydr. Lett. 3*, 17−24.
15. DiGiammarino, E. L., Draker, K., Wright, G. D., and Serpersu, E. H. (1998) *Biochemistry 37*, 3638−3644.
16. Cox, J. R., Ekman, D. R., DiGiammarino, E. L., Akal-Strader, A., and Serpersu, E. H. (2000) *Cell Biochem. Biophys.* (in press).
17. Serpersu, E. H., Cox, J. R., DiGiammarino, E. L., Mohler, M. L., Ekman, D. R., Akal-Strader, A., and Owston, M. (2000) *Cell Biochem. Biophys.* (in press).
18. Shimizu, K., Kumada, T., Hsieh, W.-C., Chung, H.-Y., Chong, Y., Hare, R. S., Miller, G. H., Sabatelli, F. J., and Howard, J. (1985) *Antimicrob. Agents Chemother. 28*, 282−288.
19. Gates, C. A., and Northrop, D. B. (1988) *Biochemistry 27*, 3820−3825.
20. Gates, C. A., and Northrop, D. B. (1988) *Biochemistry 27*, 3826−3833.
21. Gates, C. A., and Northrop, D. B. (1988) *Biochemistry 27*, 3834−3842.
22. Chen-Goodspeed, M., Vanhooke, J. L., Holden, H. M., and Raushel, F. M. (1999) *Bioorg. Chem. 27*, 395−408.
23. Ames, B. N. (1965) *Methods Enzymol. 7*, 115−118.
24. Van Pelt, J. E., Mooberry, E. S., and Frey, P. A. (1990) *Arch. Biochem. Biophys. 280*, 284−291.
25. Zwahlen, C., Vincent, S. J. F., Di Bari, L., Levitt, M. H., and Bodenhausen, G. (1994) *J. Am. Chem. Soc. 116*, 362−368.
26. Vincent, S. J. F., Zwahlen, C., and Bodenhausen, G. (1996) *J. Biomol. NMR 7*, 169−172.
27. Weiner, S. J., Kollman, P. A., Nguyen, D. T., and Case, D. A. (1986) *J. Comput. Chem. 7*, 230−252.
28. Homans, S. W., and Forster, M. (1992) *Glycobiology 2*, 143−151.
29. Yoshizawa, S., Fourmy, D., and Puglisi, J. D. (1998) *EMBO J. 17*, 6437−6448.
30. Fourmy, D., Recht, M. I., Blanchard, S. C., and Puglisi, J. D. (1996) *Science 274*, 1367−1371.
31. Gupta, R. K., Fung, C. H., and Mildvan, A. S. (1976) *J. Biol. Chem. 251*, 2421−2430.
32. Mildvan, A. S., and Gupta, R. K. (1978) *Methods Enzymol. 44G*, 322−399.
33. Villafranca, J. J. (1982) *Methods Enzymol. 87*, 180−197.
34. Wolkers, W. F., Gregory, J. D., Churchich, J. E., and Serpersu, E. H. (1991) *J. Biol. Chem. 31*, 20761−20766.
35. Gregory, J. D., and Serpersu, E. H. (1993) *J. Biol. Chem. 268*, 3880−3888.
36. Van pelt, J. E., Iyengar, R., and Frey, P. A. (1986) *J. Biol. Chem. 261*, 15995−15999.

BI002827B